

Cytotoxic and Antioxidative Effects of Geranium Oil and Ascorbic Acid Coloaded in Niosomes against MCF-7 Breast Cancer Cells

Sherif Ashraf Fahmy,¹ Soad Nasr,¹ Asmaa Ramzy, Abdelhameed S. Dawood, Anwar Abdelnaser,* and Hassan Mohamed El-Said Azzazy*



Cite This: *ACS Omega* 2023, 8, 22774–22782



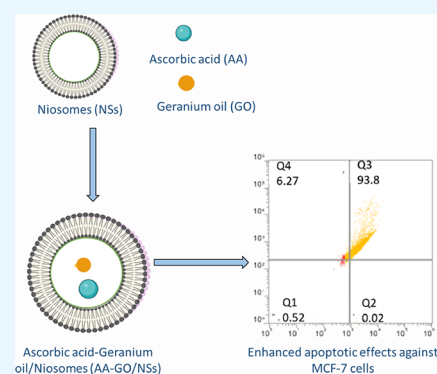
Read Online

ACCESS |

Metrics & More

Article Recommendations

ABSTRACT: Geranium oil (GO) has antiproliferative, antiangiogenic, and anti-inflammatory properties. Ascorbic acid (AA) is reported to inhibit the formation of reactive oxygen species, sensitize cancer cells, and induce apoptosis. In this context, AA, GO, and AA-GO were loaded into niosomal nanovesicles to ameliorate the physicochemical properties of GO and improve its cytotoxic effects using the thin-film hydration technique. The prepared nanovesicles had a spherical shape with average diameters ranging from 200 to 300 nm and exhibited outstanding surface negative charges, high entrapment efficiencies, and a controlled sustained release over 72 h. Entrapping AA and GO in niosomes resulted in a lower IC₅₀ value than free AA and GO when tested on MCF-7 breast cancer cells. In addition, flow cytometry analysis showed higher apoptotic cells in the late apoptotic stage upon treating the MCF-7 breast cancer cells with AA-GO niosomal vesicles compared to treatments with free AA, free GO, and AA or GO loaded into niosomal nanovesicles. Assessing the antioxidant effect of the free drugs and loaded niosomal nanovesicles showed enhanced antioxidant activity of AA-GO niosomal vesicles. These findings suggest the AA-GO niosomal vesicles as a potential treatment strategy against breast cancer, possibly through scavenging free radicals.



1. INTRODUCTION

Essential oils demonstrate various therapeutic activities, including antimicrobial, anti-inflammatory, anticancer, and antioxidant properties, owing to their high contents of monoterpenes and sesquiterpenes. Geranium oil (GO),¹ obtained by steam distillation of the leaves of *Pelargonium graveolens*, is one of these promising medicinal essential oils. Previous studies reported the antiproliferative, antiangiogenic, and anti-inflammatory properties of GO in metastatic cancer cell lines.² The main constituents of GO, including geraniol, citronellol, and citronellyl formate, were reported to have antioxidant activity and remarkable antiproliferative activity against different cancer cell lines.^{3,4}

Ascorbic acid (AA, vitamin C) is a necessary human nutrient with pronounced antioxidant activity that shields cellular constituents from the devastating effects of free radicals and is a cofactor in various enzymatic reactions.⁵ In addition, AA has been reported to selectively kill cancer cells *in vitro* and slow the growth of a variety of human tumor xenografts in immunocompromised mice.⁶ Additionally, AA functions as a chemosensitizer that sensitizes cancer cells to different synthetic and natural anticancer drugs, enhancing their anticancer effects.¹¹ AA is a low-molecular-weight antioxidant that inhibits the formation of reactive oxygen species (ROS) levels. Another way that AA prevents oxidative stress is the

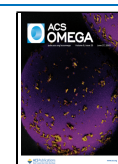
significant stimulation of the cellular antioxidant system and the generation of other low-molecular-weight antioxidants.⁷ Some studies have shown the synergistic effects of AA in combination with other natural products in inducing cancer cell death. Even though the mechanism by which AA induces apoptosis is still not fully understood, some studies reported that AA treatment increased Bax (proapoptotic) protein expression and upregulates p53 (tumor suppression) gene expression, which induces apoptosis.⁸

Despite the broad therapeutic activities of essential oils, their clinical application is challenged by their limited water solubility, poor pharmacokinetics, and low potency resulting from nonselective delivery to the target tissue. Thus, various nanocarrier systems were developed for encapsulating essential oils and other natural compounds to improve their water solubility and therapeutic activities. These include supramolecules,^{9,10} polymeric nanocomposites,^{11,12} and lipid nanovesicles (including liposomes and niosomes).^{13,14} Niosomes

Received: March 13, 2023

Accepted: May 12, 2023

Published: June 13, 2023



(NSs) are amphiphilic nanostructures designed by the self-assembly of nonionic surfactants and cholesterol in an aqueous medium, forming bilayer-closed nanovesicles.¹⁴ Several methods are used to generate niosomes; however, thin-film hydration followed by sonication is commonly used due to its simplicity.¹⁵ Using niosomes to deliver various therapeutic drugs offers many advantages as they are stable, affordable, biocompatible, and biodegradable.^{14,15} Previous studies reported using niosomal vehicles to deliver several chemotherapeutics and antioxidant drugs.^{16,17} Targeted delivery of drugs using niosomes can be achieved passively (due to enhanced permeation and retention of niosomes in tumors) or actively by modifying the surface of niosomes to release their payloads in response to different stimuli such as a magnetic field or pH.¹⁸

This study aimed to explore the enhanced anticancer and antioxidant activities of GO and AA when they are co-loaded in niosomal nanovesicles. In this regard, AA/NSs, GO/NSs, and AA-GO/NSs were prepared using the thin-film hydration method. Then, the prepared niosomes were characterized in terms of size, PDI, surface charge, morphology, and entrapment efficiency. In addition, the *in vitro* release profiles of the prepared niosomal formulations were investigated at low pH typical of the cancer microenvironment. Moreover, the effects of free AA, free GO, AA/NSs, GO/NSs, and AA-GO/NSs on MCF-7 cells were investigated. The apoptotic and antioxidative stress effects of the niosomal formulations on MCF-7 cells were assessed.

2. MATERIALS AND METHODS

2.1. Materials. Cholesterol, Span 60, and Tween 60 were acquired from Biosynth Carbosynth, Berkshire, UK. Geranium oil was purchased from a local company (Imtenan, Cairo, Egypt). Ascorbic acid was obtained from Sigma-Aldrich (St. Louis, MO, USA). Dulbecco's modified Eagle's medium (DMEM) containing glucose (4.5 g/L), trypsin (0.05%), and phosphate-buffered saline (PBS, pH 7.4), penicillin–streptomycin, and 3-(4,5-dimethylthiazol-2-yl)-2,5-diphenyltetrazolium bromide (MTT) were purchased from Lonza Bioscience (Walkersville, MD, USA). Fetal bovine serum (FBS) was obtained from Gibco (Waltham, MA, USA). Dimethyl sulfoxide (DMSO) was acquired from Serva (Heidelberg, Germany). 2',7'-Dichlorodihydrofluorescein diacetate (H2DCFDA) was purchased from Invitrogen-Thermo Fisher Scientific (Waltham, USA), and an Annexin V-FITC/7-AAD apoptosis detection kit (cat. no. E-CK-A212.50) was purchased from Elabscience (Wuhan, China). Propidium iodide (PI) was purchased from Invitrogen (Waltham, MA, USA). All other chemicals were purchased from Sigma-Aldrich. The MCF-7 cell line (cat. no. HTB-22) was purchased from ATCC (Manassas, VA, USA).

2.2. Preparation of Niosomes (NSs). NSs loaded with AA (AA/NSs), GO (GO/NSs), or AA-GO (AA-GO/NSs) were prepared using the thin-film hydration technique with some modifications.^{15,19} In order to prepare AA-GO/NSs, a total of 120 mmol of cholesterol, Span 60, and Tween 60 was used in a molar ratio of 2:1:1. Briefly, the cholesterol, surfactants, and GO were dissolved in chloroform. The organic solvent was then evaporated under reduced pressure for 60 min at 60 °C, utilizing a rotary evaporator (Laborota 4000, Heidolph Instruments, Schwabach, Germany) equipped with a vacuum pump (KNF Neuberger GmbH, Freiburg, Germany), leaving a thin lipid film. AA was dissolved in phosphate-

buffered saline (PBS, pH 7.4) and then was used to hydrate the thin film in a rotary evaporator under normal pressure at the same temperature for 60 min. The obtained suspension was sonicated for 5 min using a bath sonicator (Elmasonic P30 H, Elma Hans Schmidbauer, Singen, Germany). Blank NSs were prepared using the same method without adding GO or AA. Then, the prepared suspensions were left for 45 min at room temperature and then kept at 4 °C for further investigation.

2.3. Characterization of the Niosomal Preparations.

The average particle size, PDI, and zeta potential were measured employing a Zetasizer Nano ZS equipped with a 10 mW HeNe laser (Malvern Instruments, Worcestershire, UK). Size measurement was conducted in triplicate at 25 °C. The morphological features of the GO/NSs, AA/NSs, and GO/AA/NSs were evaluated using high-resolution field emission scanning electron microscopy (FESEM, LEO SUPRA 55, Carl Zeiss, Oberkochen, Germany) using an acceleration voltage of 1.00 kV. All freeze-dried samples were subjected to gold sputtering at 10 mA for 2 min under nitrogen before carrying out FESEM analysis. The FTIR spectra of AA, GO, plain niosomes, AA/NSs, GO/NSs, and AA-GO/NSs were studied utilizing attenuated total reflection Fourier-transform infrared spectroscopy (ATR-FTIR) using an FTIR Nicolet 380 spectrometer (Thermo Scientific, Waltham, MA), equipped with a ZnSe flat crystal (in the range of 4000 and 650 cm^{-1}).

2.4. Niosome Entrapment Efficiency. The entrapment efficiency percentages (EE %) of the loaded AA and/or GO into niosomes (AA/NSs, GO/NSs, and AA-GO/NSs) were determined as described previously with minor modifications.²⁰ Briefly, 1 mL of each formula was centrifuged at 10,000 rpm and 4 °C for 2 h to remove free AA and/or GO. Then, the supernatant was aspirated and used to measure the free AA and GO using a UV–vis spectrophotometer (FLUOstar Omega microplate reader, BMG Labtech, Offenburg, Germany) at 252 and 244 nm, respectively. The EE % was computed using eq 1.

$$\text{EE\%} = \frac{\text{the initial amount of the drug or oil} - \text{the amount of oil}}{\text{the initial amount of oil}} \times 100 \quad (1)$$

2.5. *In Vitro* Release Study. The release rates of AA and GO from AA/NSs, GO/NSs, and AA-GO/NSs were studied employing the dialysis membrane approach at pH 7.4 and 5.5. Briefly, 0.5 mL of the niosomal preparation was pipetted into a dialysis bag (12–14 KD cutoff), which was then placed in a beaker containing 25 mL of PBS (adjusted at pH values of 7.4 or 5.5). Then, the beaker was placed in a shaking incubator (Jeio Tech SI-300, Seoul, Korea), rotating at 150 rpm at 37 ± 0.5 °C. At specific time points, 1 mL aliquots of the sample were withdrawn for quantification of AA and GO by UV–vis spectrophotometry (at 252 and 244 nm, respectively) and immediately replaced with another 1 mL of warmed buffer. The release % of AA and GO was determined using eq 2.

$$\text{release\%} = \frac{\text{the amount of released oil}}{\text{the initial amount of loaded oil}} \times 100 \quad (2)$$

2.6. Cell Viability Assay. MCF-7 breast cancer cells were cultured in DMEM at 37 °C in a 5% CO_2 humidified incubator. DMEM was supplemented with 1% pen–strep (100 units/mL penicillin and 100 $\mu\text{g}/\text{mL}$ streptomycin) and 10% heat-inactivated FBS. MCF-7 cells were then seeded in a 96-well plate at a density of 10,000 cells/well. The next day,

Table 1. Characteristics of Different Niosomal Formulas^a

samples	diameter (nm)	PDI	ζ potential (mV)	EE (%)	
				GO	AA
plain NSs	231.2 \pm 41.3	0.21 \pm 0.17	-6.39 \pm 1.96		
GO/NSs	210.3 \pm 35.0	0.24 \pm 0.16	-9.81 \pm 1.12	98.1 \pm 5.1	
AA/NSs	204.5 \pm 29.8	0.19 \pm 0.13	-7.45 \pm 1.23		99.5 \pm 2.3
GO-AA/NSs	219.4 \pm 44.5	0.23 \pm 0.20	-11.1 \pm 1.39	98.3 \pm 4.2	98.7 \pm 3.1

^aAll experiments were conducted in triplicate, and the results were expressed as means \pm standard deviations. AA: ascorbic acid, GO: geranium oil, and NSs: niosomes.

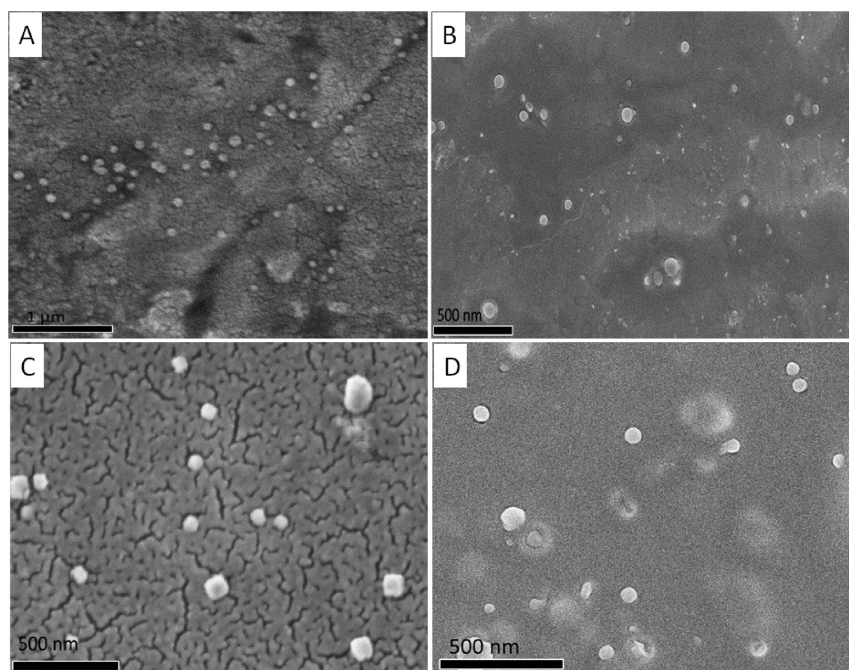


Figure 1. Scanning electron microscopy (SEM) micrographs of (A) plain NSs, (B) AA/NSs, (C) GO/NSs, and (D) AA-GO/NSs.

cultured cells were treated with free AA dissolved in PBS, free GO dissolved in DMSO, AA/NSs, GO/NSs, AA-GO/NSs, plain niosomes, or doxorubicin (DOX) as a positive control with increasing concentrations in basal media. After another 24 h, the supernatant was discarded, and MTT solution (1 mg/mL) was added to cells and left for 2 h at 37 °C and then discarded. DMSO (100 μ L) was added to the cultured cells to solubilize the formed formazan crystals. Finally, absorbance was measured at 540 nm using a TECAN microplate reader (Infinite 200 Pro, Männedorf, Switzerland). As compared to the control, the percentage of viable cells in treated wells was calculated. The viability inhibition concentrations at 50% (IC_{50}) were then calculated using GraphPad Prism 9.0 (San Diego, CA, USA) by plotting absorbance data against the concentrations tested for each sample.

2.7. Cell Apoptosis Assay Using Flow Cytometry. MCF-7 cells were seeded in T-25 flasks (5×10^2 cells per flask) and incubated at 37 °C for 24 h. The next day, cultured cells were treated with IC_{50} concentrations of different treatments, as prepared above, in basal media. After another 24 h of treatment, cells were collected and prepared for flow cytometry measurements using an Annexin V-FITC/7-AAD apoptosis detection kit according to manufacturer's procedures. MCF-7 cell apoptosis was evaluated using flow cytometry (Attune NxT, Thermo Fisher Scientific).²¹ Analysis

of flow cytometry data was performed using FlowJo software version 10.6.2 (Ashland, OR, USA).

2.8. Reactive Oxygen Species Assay. A fluorometric assay was used to measure ROS levels induced by AA, GO, AA/NSs, GO/NSs, AA-GO/NSs, and plain niosomes by using the intracellular oxidation of 2',7'-dichlorofluorescein diacetate (DCF-DA). MCF-7 cells were seeded in 96-well plates at a density of 1×10^3 cells/well and left overnight. The cultured cells were then pretreated with 100 μ L of 5 μ M DCF-DA in basal medium for 2 h. Then, 100 μ L of each treatment was added at a concentration half that of the IC_{50} value bringing the total volume of 200 μ L. After 24 h of incubation in the dark, fluorescence was measured using excitation and emission wavelengths of 485 and 535 nm, respectively. Fluorescence measurement was performed using a TECAN microplate reader Infinite 200 Pro (Männedorf, Switzerland).

2.9. Statistical Analysis. All measurements were performed in triplicates, and standard deviations (SD) were calculated. One-way ANOVA was performed using GraphPad Prism v 8.0 (GraphPad, San Diego, CA, USA). A *P*-value of <0.05 was considered statistically significant.

3. RESULTS AND DISCUSSION

3.1. Characteristics of the Prepared Niosomal Formulations. The average diameters and PDI of AA/NSs, GO/NSs, and AA-GO/NSs were measured using dynamic

light scattering (Table 1). The average diameters of all fabricated niosomal nanovesicles were between 200 and 300 nm, which agrees with a previous study that reported the formulation of various nanostructures loaded with anticancer drugs and exhibited potent anticancer activities.²² This nanoscale range aids the passive accumulation of the loaded drugs into cancer cells via preferential diffusion through the leaky vasculature of cancer tissues.²² As shown in Table 1, the surface charges of the designed nanovesicles were -6.39 ± 1.96 , -9.81 ± 1.12 , -7.45 ± 1.23 , and -11.1 ± 1.39 mV for plain NSs, AA/NSs, GO/NSs, and AA-GO/NSs, respectively. These negative surface charges minimize the nanovesicles' agglomeration and prolong their shelf lives. The entrapment efficiency percentages (EE %) of the three prepared nanovesicles demonstrate the capability of niosomal vesicles to encapsulate large amounts of either AA, GO, or AA-GO (Table 1). These findings showed that the hydrophilic AA and the hydrophobic GO are well-settled in the aqueous niosomal core and the outer niosomal lipid bilayer, respectively.

SEM analysis showed a spherical morphology for plain niosomes, AA/NSs, GO/NSs, and AA-GO/NSs (Figure 1). Loading either AA, GO, or AA-GO inside the niosomes has not impacted their spherical shape.

FTIR spectra of GO, AA, empty NSs, GO/NSs, AA/NSs, and AA-GO/NSs are presented in Figure 2. The ATR-FTIR spectrum of GO (Figure 2A) revealed three main peaks at 3373.7 (–OH stretching), 2925.9 (–CH₃ stretching), and 1729.7 (C=O stretching). Furthermore, the ATR-FTIR

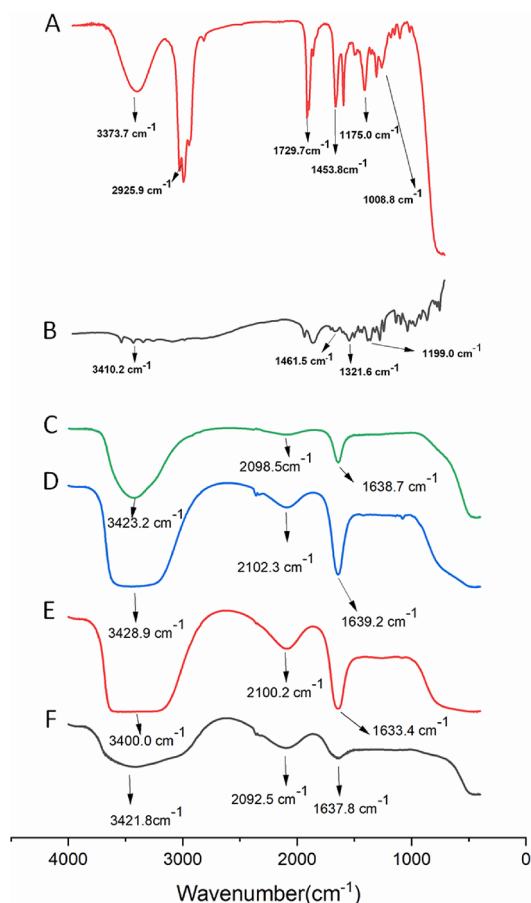


Figure 2. FTIR spectra of (A) GO, (B) AA, (C) plain niosomes, (D) AA/NSs, (E) GO/NSs, and (F) AA-GO/NSs.

spectrum of AA (Figure 2B) demonstrated four distinct peaks at 3410.2 (–OH stretching), 1416.5, 1321.6 (–CH bending), and 1199.0 cm⁻¹ (C–O–C stretching). The spectrum of plain NSs (Figure 2C) exhibited three major peaks at 3423.2 (–OH stretching), 2098.5, and 1638.7 cm⁻¹ (C=C stretching). On the other hand, the spectra of GO/NSs, AA/NSs, and AA-GO/NSs demonstrated the disappearance of three characteristic peaks of GO, which are at 2925.9 (–CH₃ stretching), 1729.7 (C=O stretching), and 1453.8 cm⁻¹ (C–H bending). Also, the disappearance of AA's characteristic peaks, 1416.5 and 1321.6 cm⁻¹ (–CH bending), confirms the GO's and AA's successful entrapment within the niosomal matrix.²³

3.2. In Vitro Release Study. The release study was conducted in acidic media (pH of 5.5) to simulate the acidic conditions inside the tumor microenvironment and/or intracellular endosomes. The release percentage of AA and GO from the niosomal nanovesicles was studied at 37 °C and pH 5.5 (tumor cells' extracellular pH), as presented in Figure 3. The release % values of AA and GO from AA/NSs and GO/NSs, after 72 h in acidic media, were 80.85 ± 2.8 and 76.80 ± 1.79 , respectively. On the other hand, the release % values of AA and GO from AA-GO/NSs were found to be 76.1 ± 3.1 and 71.83 ± 1.87 , respectively. The release study showed that the release % values of the coloaded drugs (AA-GO) from AA-GO/NSs (80.85 ± 2.8 and 76.80 ± 1.79 , respectively) were not decreased significantly ($p < 0.5$) as compared to that of AA (76.1 ± 3.1) and GO (71.83 ± 1.87) from AA/NSs and GO/NSs, respectively. In addition, all formulations have shown a sustained release behavior where about 72–80% of the loaded drugs were released over a period of 72 h. This sustained release manner is attributed to the presence of cholesterol, which improves the stability of the outer bilayer membrane of the niosomes and, thus, minimizes the leakage of the entrapped AA or GO outside the niosomal membranes.²⁴ Therefore, high amounts of loaded AA and GO could be delivered to the site of action over a prolonged time, supporting the anticancer potential of the developed niosomal preparations.

3.3. Cell Viability Assay. Breast cancer is one of the most commonly diagnosed cancers in women worldwide, accounting for approximately 30% of all cancer diagnoses.²⁵ MCF-7 cells are a well-established and widely used breast cancer cell line that has been extensively characterized and validated for studying breast cancer.²⁶ On the other hand, GO has been reported previously to suppress tumor progression in breast cancer and enhance the cytotoxicity of tamoxifen.^{27,28} Additionally, AA has been reported to promote apoptosis in breast cancer cells.²⁹ In this regard, MCF-7 cells were treated for 24 h using increasing concentrations (1.25, 2.5, 5, 10, 20, 40, 80, 160, and 320 μg/mL) of free AA, free GO, or AA and GO loaded in AA/NSs, GO/NSs, or AA-GO/NSs, in addition to plain niosomes and DOX. The cell viability assay was evaluated using the MTT assay. Figure 4 illustrates that AA dissolved in PBS alone had an IC₅₀ value of 20.5 ± 13 μg/mL. However, when AA is entrapped into niosome nanovesicles, the IC₅₀ value slightly decreases (18.97 ± 6 μg/mL). GO dissolved in DMSO alone had an IC₅₀ value of 65.63 ± 14 μg/mL. However, when GO was encapsulated in niosomal nanovesicles, the IC₅₀ significantly decreased to 47.46 ± 11 μg/mL ($P < 0.01$), indicating higher potency in reducing the viability of cancer cells. The combination of AA and GO in niosomes showed the lowest IC₅₀ of 9.2 ± 8 μg/mL, thus indicating the highest anticancer potential. Lastly, to ensure that the cytotoxicity is due to the active ingredient and not

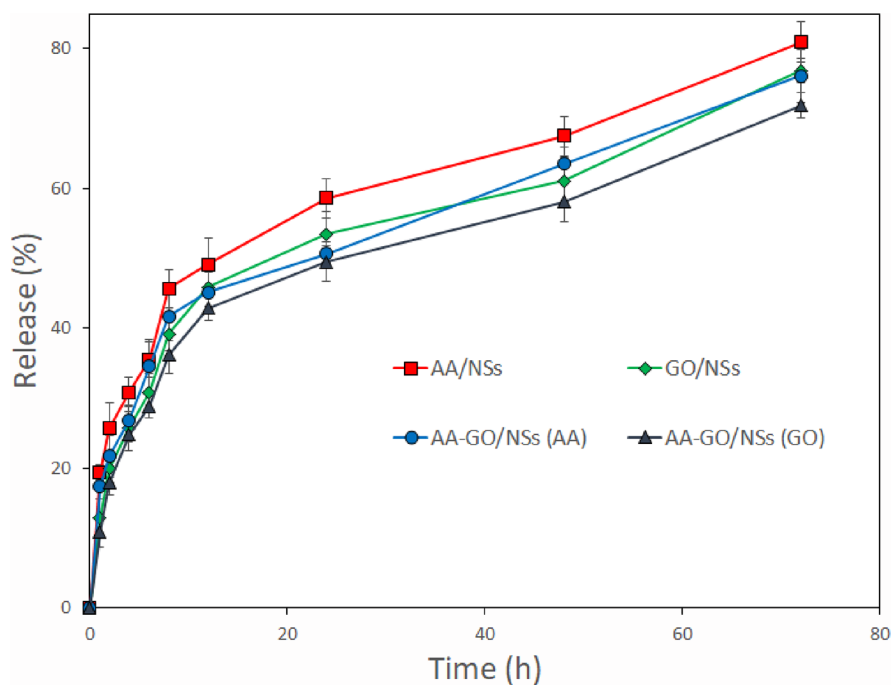


Figure 3. *In vitro* release profile of AA and GO from AA/NSs, GO/NSs, and AA-GO/NSs at 37 °C and pH 5.5. Concentrations were deduced from eq 2 after measuring the absorbance of AA and GO at 252 and 244 nm, respectively.

attributed to the nonionic surfactant content of the niosome carrier, the effect of blank niosomes was tested on cellular viability. Plain NSs had an IC_{50} of $125.25 \pm 9 \mu\text{g/mL}$, which was significantly higher than the loaded nanocarriers, AA/NSs, GO/NSs, and AA-GO/NSs. In addition, plain niosomes exhibited minimal or no cytotoxicity on the MCF-7 cells compared to untreated cells (negative control). These results agree with a previous report concerning the minimal cytotoxic effects of niosomes on MCF-7 cells.³⁰ Lastly, to ensure that the assay is functioning correctly and provides a reference point for interpreting the results of the test compound, we tested DOX cytotoxicity and calculated its IC_{50} (Table 2). Our results demonstrated that DOX had an IC_{50} value of $3.48 \mu\text{g/mL}$. Our results are consistent with previously published reports in which DOX had an IC_{50} value ranging from 1.2 to $5.1 \mu\text{g/mL}$.³¹ The encapsulation of AA and GO in the niosomes would lead to enhanced accumulation of the AA and GO inside cancer cells.³² The combination of AA and GO encapsulated in niosomes showed enhanced cytotoxicity against MCF-7 cells, suggesting an enhanced anticancer activity that may be due to a synergistic effect of the active ingredients in comparison to AA/NSs and GO/NSs alone.³³ Encapsulation of AA in niosomes has led to increased toxicity (lower IC_{50}) as compared to AA in PBS. This may be due to the fact that niosomes facilitate cellular uptake of their contents due to their lipid-based structure that can easily fuse with cell membranes. This leads to improved intracellular accumulation of loaded drugs and a consequent increase in their cytotoxicity. Also, niosomes could facilitate the controlled release of their payloads within the MCF-7 cells. This can cause a sustained and prolonged effect of either AA or GO, contributing to its increased cytotoxicity.^{29–31} On the other hand, niosomes can improve the stability of their cargos, protecting them from degradation by enzymes and other factors, resulting in higher concentrations of either active AA or GO being available to exert its cytotoxic effect.^{34–36}

3.4. Apoptosis Assay. The apoptotic effects of the tested compounds on MCF-7 cells were examined using flow cytometry. In the cell viability assay, encapsulating AA and GO in niosomal nanovesicles, either alone or in combination, showed enhanced cytotoxic effects against MCF-7 cells. It was important to test whether free AA, GO, or AA and AA/NSs, GO/NSs, AA-GO/NSs, and plain niosomes could exhibit similar behavior in the apoptosis assay. IC_{50} concentrations that were determined by the MTT assay were used for the cell apoptosis assay. Percentages of apoptotic cells were determined using flow cytometric analysis by Annexin/PI staining as previously described.³⁷ Results show that treatment with the niosomal active ingredients exhibited variable effects on the percentages of early and late apoptotic cells. After 24 h of treatment, AA alone induced mostly late apoptosis. The percentages of viable, early apoptotic, and late apoptotic cells were 3.79, 0, and 80.7%, respectively (Figure 5). AA/NSs also showed similar percentages of viable, early apoptotic, and late apoptotic cells (3.85, 0, and 79.1%, respectively). For GO alone, the percentages of viable, early apoptotic, and late apoptotic percentages were 2.19, 0.03, and 84.1%, respectively. For GO/NSs, the results for the cell apoptosis assay were also similar with 2.12, 0, and 87.3% of viable, early apoptotic, and late apoptotic cells, respectively. However, when AA and GO were combined and encapsulated into niosomal nanovesicles, the percentage of viable cells decreased to 0.52%, and that of late apoptotic cells increased to 93.8%, compared to the control, which had a cell viability of 98.8%. The percentage of early apoptotic cells for all tested samples remained close to 0%. This may be attributed to the long treatment strategy so that the late apoptosis stage was greatly increased.³⁸ Plain niosomes induced the least apoptotic effect of 61.2% for late apoptotic cells. In a previous study, AA has been shown to induce intrinsic apoptotic pathways in colorectal carcinoma cells.³⁹ In addition, GO in a previous study repressed cell viability in MCF-7 cells and induced apoptosis.²⁷ The results

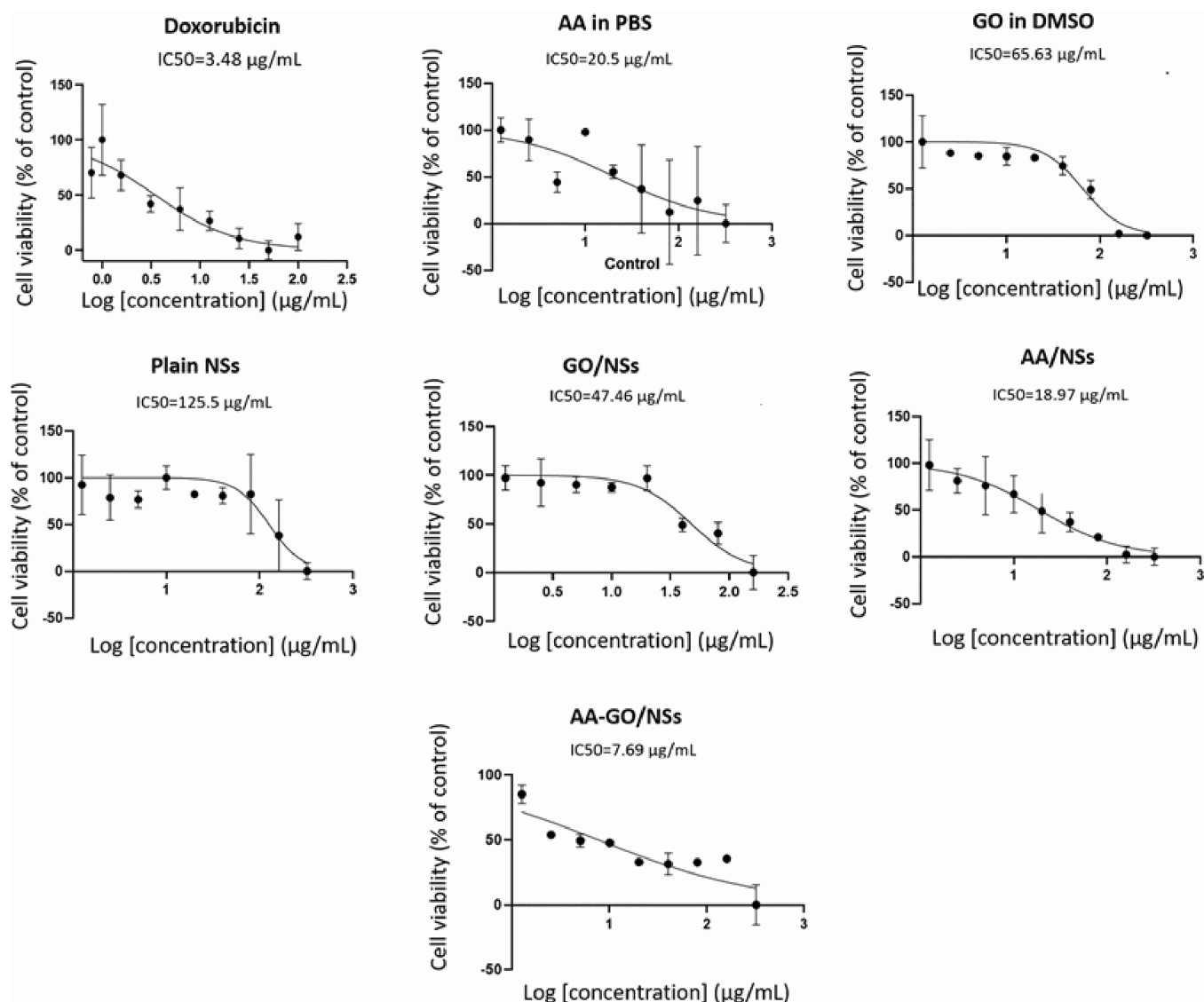


Figure 4. Determination of IC_{50} values of geranium oil (GO), ascorbic acid (AA), and doxorubicin (DOX) on MCF-7 cells. Increasing concentrations (1.25, 2.5, 5, 10, 20, 40, 80, 160, and 320 $\mu\text{g/mL}$) of free AA, free GO, or AA and GO loaded in AA/NSs, GO/NSs, AA-GO/NSs, and plain niosomes (NSs) were prepared for calculations of IC_{50} values. The MTT assay was used for cellular viability measurements. Values are means \pm SD ($n = 3$).

Table 2. IC_{50} Values of Free and Encapsulated Geranium Oil and Ascorbic Acid

sample name	IC_{50} ($\mu\text{g/mL}$)
AA in PBS	20.5 ± 13
AA/NSs	18.97 ± 6
GO in DMSO	65.63 ± 14
GO/NSs	47.46 ± 11
AA-GO/NSs	7.69 ± 8
plain NSs	125.5 ± 9
DOX	3.48 ± 17

confirmed that MCF-7 cells treated with AA/NSs and GO/NSs had significantly higher apoptotic cells ($p < 0.001$) than those observed in cells treated with plain niosomes or untreated control cells. In addition, our results indicated that a combination of AA and GO encapsulated in niosomal nanovesicles significantly ($p < 0.01$) enhanced their apoptotic

effect as compared to the effects of either AA or GO encapsulated in niosomes.

3.5. Determination of ROS. ROS production was determined using the fluorogenic dye H2DCFDA (Figure 6). The dye diffuses typically into the cell, where it is deacetylated by cellular esterases into a nonfluorescent compound. Afterward, intracellular ROS oxidizes the compound into 2',7'-dichlorofluorescein (DCF).^{40,41} Treatment of MCF-7 with half of IC_{50} of free AA or GO or AA and GO encapsulated in AA/NSs, GO/NSs, AA-GO/NSs, and plain niosomes for 24 h was conducted to determine the ability of the tested compounds to convert H2DCFDA to its fluorescent product DCF. The tested compounds caused a significant decrease in fluorescence in comparison to the control, indicating a reduction in ROS production after treatment. A combination of AA and GO encapsulated in niosomal nanovesicles showed the most significant decrease in fluorescence in comparison to the other treatments. Empty niosomes showed the least decrease in fluorescence, indicating the lowest antioxidative

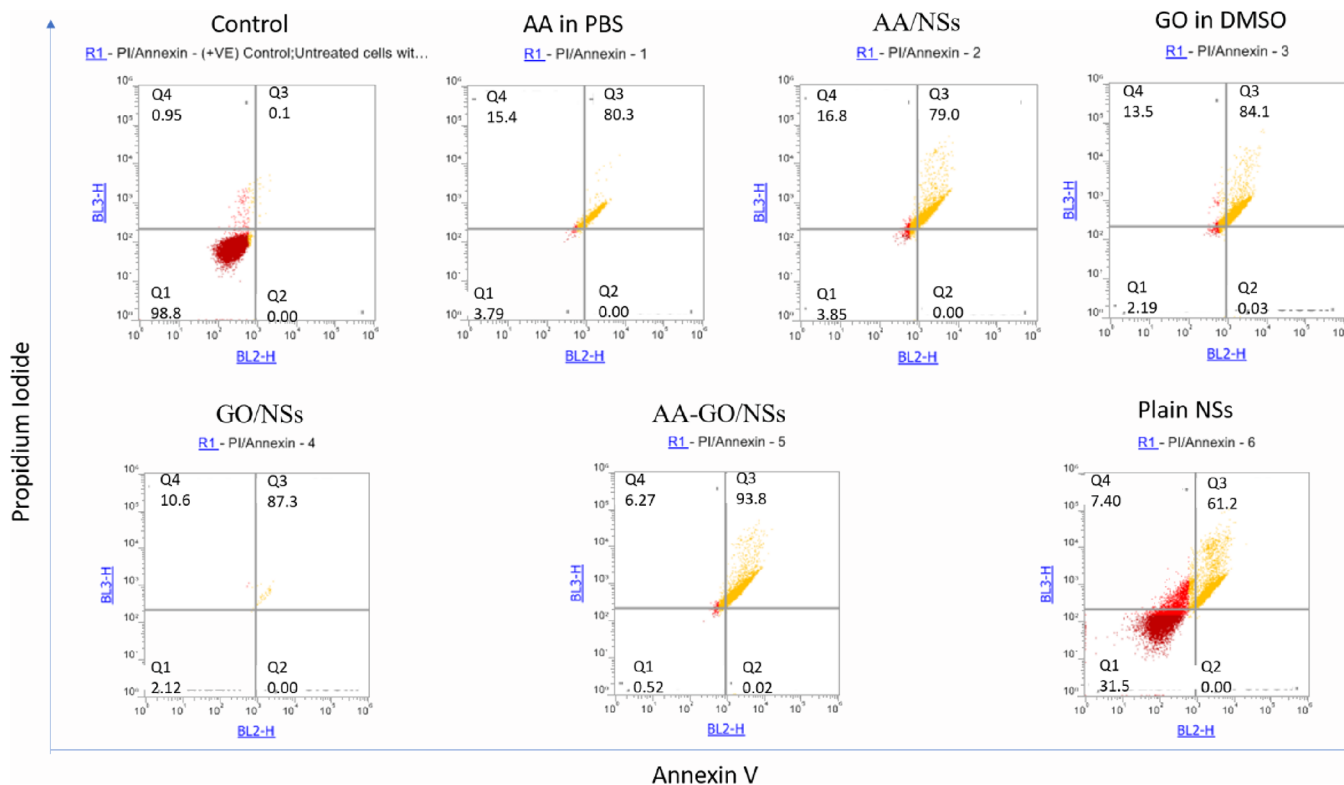


Figure 5. Cell apoptosis assay using flow cytometry of free and encapsulated ascorbic acid (AA) and geranium oil (GO). MCF-7 cells were treated for 24 h with IC₅₀ concentrations of free AA, free GO, AA/NSs, GO/NSs, AA-GO/NSs, and empty niosomes. Percentages of viable cells and early and late apoptotic cells were then determined using Annexin/PI staining.

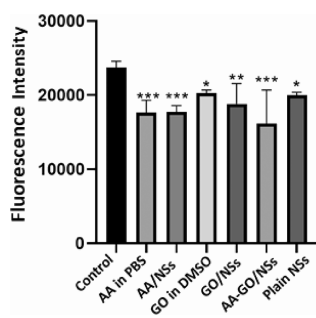


Figure 6. Evaluation of ROS level production using the fluorogenic dye H₂DCFDA. MCF-7 cells were treated for 24 h with free AA, GO, AA/NSs, GO/NSs, AA-GO/NSs, or plain niosomes using concentrations half those of respective IC₅₀ values. Fluorescence intensity was then measured upon excitation at 485 and measuring emission at 535 nm. Data are presented as means \pm SD. * p < 0.01, ** p < 0.05, and *** p < 0.001.

stress properties against MCF-7 cells. It is of note that AA was reported to reduce ROS levels.⁴²

4. CONCLUSIONS

Niosomal nanovesicles encapsulating AA and/or GO were fabricated by the thin-film hydration method. All formulas showed a nanoscale size range of 200–300 nm, low PDI, outstanding zeta potential, and high EE %. The ability to entrap high concentrations of AA and GO supports the improved anticancer and antioxidant activities of the prepared niosomes. *In vitro* release studies demonstrated the capability of the prepared nanovesicles to sustainably release their cargo in the acidic microenvironment of cancer tissues (pH 5.5) over

72 h. Combining AA and GO in niosomal nanovesicles led to enhanced cytotoxicity and an increased early apoptotic effect on MCF-7 cells. In addition, AA-GO niosomal nanovesicles exhibited enhanced antioxidative activity in comparison to free AA, free GO, and AA and GO loaded individually or in combination in niosomal nanovesicles. Loading GO and AA in niosomes showed enhanced anticancer properties against MCF-7 breast cancer cells, which warrants further investigations of its possible utility for the treatment of breast cancer.

AUTHOR INFORMATION

Corresponding Authors

Anwar Abdelnaser – Institute of Global Health and Human Ecology, School of Sciences & Engineering, The American University in Cairo, New Cairo 11835, Egypt;
Email: anwar.abdelnaser@aucegypt.edu

Hassan Mohamed El-Said Azzazy – Department of Chemistry, School of Sciences & Engineering, The American University in Cairo, New Cairo 11835, Egypt; Department of Nanobiophotonics, Leibniz Institute for Photonic Technology, Jena 07745, Germany; orcid.org/0000-0003-2047-4222;
Email: hazzazy@aucegypt.edu

Authors

Sherif Ashraf Fahmy – Chemistry Department, School of Life and Medical Sciences, University of Hertfordshire Hosted by Global Academic Foundation, Cairo 11835, Egypt; Department of Chemistry, School of Sciences & Engineering, The American University in Cairo, New Cairo 11835, Egypt; orcid.org/0000-0003-3056-8281

Soad Nasr – Institute of Global Health and Human Ecology, School of Sciences & Engineering, The American University in Cairo, New Cairo 11835, Egypt

Asmaa Ramzy – Department of Chemistry, School of Sciences & Engineering, The American University in Cairo, New Cairo 11835, Egypt

Abdelhameed S. Dawood – Institute of Global Health and Human Ecology, School of Sciences & Engineering, The American University in Cairo, New Cairo 11835, Egypt

Complete contact information is available at:

<https://pubs.acs.org/10.1021/acsomega.3c01681>

Author Contributions

[†]S.A.F. and S.N. contributed equally to this work.

Notes

The authors declare no competing financial interest.

ACKNOWLEDGMENTS

This work is funded by a grant from the American University in Cairo to Prof. Hassan Azzazy. It is funded by grants from ASRT (Jesor) and the American University to Dr. Anwar Abdelnaser.

REFERENCES

- (1) Fayed, S. Antioxidant and Anticancer Activities of Citrus reticulata (Petitgrain mandarin) and Pelargonium graveolens (Geranium) Essential Oils. *Res. J. Agric. Biol. Sci.* **2009**, *5*, 740–747.
- (2) Boukhatem, M. N.; Sudha, T.; Darwish, N. H. E.; Nada, H. G.; Mousa, S. A. Rose-scented geranium essential oil from Algeria (Pelargonium graveolens L'Herit.): Assessment of antioxidant, anti-inflammatory and anticancer properties against different metastatic cancer cell lines. *Ann. Pharm. Fr.* **2022**, *80*, 383–396.
- (3) Dzamic, A. M.; Sokovic, M. D.; Ristic, M. S.; Grujic, S. M.; Mileski, K. S.; Marin, P. D. Chemical composition, antifungal and antioxidant activity of Pelargonium graveolens essential oil. *J. Appl. Pharm. Sci.* **2014**, *4*, 001–005.
- (4) Elansary, H. O.; Abdelgaleil, S. A. M.; Mahmoud, E. A.; et al. Effective antioxidant, antimicrobial and anticancer activities of essential oils of horticultural aromatic crops in northern Egypt. *BMC Complement Altern. Med.* **2018**, *18*, 214.
- (5) Du, J.; Cullen, J. J.; Buettner, G. R. Ascorbic acid: chemistry, biology and the treatment of cancer. *Biochim. Biophys. Acta* **2012**, *1826*, 443–457.
- (6) Chen, Q.; Espey, M. G.; Krishna, M. C.; Mitchell, J. B.; Corpe, C. P.; Buettner, G. R.; Shacter, E.; Levine, M. Pharmacologic ascorbic acid concentrations selectively kill cancer cells: action as a pro-drug to deliver hydrogen peroxide to tissues. *Proc. Natl. Acad. Sci. U. S. A.* **2005**, *102*, 13604–13609.
- (7) Gęgotek, A.; Skrzydlewska, E. Antioxidative and Anti-Inflammatory Activity of Ascorbic Acid. *Antioxidants* **2022**, *11*, 1993.
- (8) Sunil Kumar, B. V.; Singh, S.; Verma, R. Anticancer Potential of Dietary Vitamin D and Ascorbic Acid: A Review. *Crit. Rev. Food Sci. Nutr.* **2017**, *2623*.
- (9) Fahmy, S. A.; Issa, M. Y.; Saleh, B. M.; Meselhy, M. R.; Azzazy, H. M. E.-S. Peganum Harmala Alkaloids Self-Assembled Supramolecular Nanocapsules with Enhanced Antioxidant and Cytotoxic Activities. *ACS Omega* **2021**, *6*, 11954–11963.
- (10) Fahmy, S. A.; Ponte, F.; Fawzy, I. M.; Sicilia, E.; Azzazy, H. M. E. S. Betaine host–guest complexation with a calixarene receptor: enhanced in vitro anticancer effect. *RSC Adv.* **2021**, *11*, 24673–24680.
- (11) Azzazy, H. M. E.-S.; Fahmy, S. A.; Mahdy, N. K.; Meselhy, M. R.; Bakowsky, U. Chitosan-Coated PLGA Nanoparticles Loaded with Peganum harmala Alkaloids with Promising Antibacterial and Wound Healing Activities. *Nanomaterials* **2021**, *11*, 2438.
- (12) Fahmy, S. A.; Mahdy, N. K.; Al Mulla, H.; ElMeshad, A. N.; Issa, M. Y.; Azzazy, H. M. E.-S. PLGA/PEG Nanoparticles Loaded with Cyclodextrin-Peganum harmala Alkaloid Complex and Ascorbic Acid with Promising Antimicrobial Activities. *Pharmaceutics* **2022**, *14*, 142.
- (13) Fahmy, S. A.; Azzazy, H. M. E.-S.; Schaefer, J. Liposome Photosensitizer Formulations for Effective Cancer Photodynamic Therapy. *Pharmaceutics* **2021**, *13*, 1345.
- (14) Fahmy, S. A.; Ramzy, A.; Sawy, A. M.; Nabil, M.; Gad, M. Z.; El-Shazly, M.; Aboul-Soud, M. A. M.; Azzazy, H. M. E.-S. Ozonated Olive Oil: Enhanced Cutaneous Delivery via Niosomal Nanovesicles for Melanoma Treatment. *Antioxidants* **2022**, *11*, 1318.
- (15) Momekova, D. B.; Gugleva, V. E.; Petrov, P. D. Nano-architectonics of Multifunctional Niosomes for Advanced Drug Delivery. *ACS Omega* **2021**, *6*, 33265–33273.
- (16) Sahrayi, H.; Hosseini, E.; Karimifard, S.; Khayam, N.; Meybodi, S. M.; Amiri, S.; Bourbour, M.; Farasati Far, B.; Akbarzadeh, I.; Bhia, M.; Hoskins, C.; Chaiyasut, C. Co-Delivery of Letrozole and Cyclophosphamide via Folic Acid-Decorated Nanoniosomes for Breast Cancer Therapy: Synergic Effect, Augmentation of Cytotoxicity, and Apoptosis Gene Expression. *Pharmaceutics* **2022**, *15*, 6.
- (17) Gugleva, V.; Michailova, V.; Mihaylova, R.; Momekov, G.; Zaharieva, M. M.; Najdenski, H.; Petrov, P.; Rangelov, S.; Forys, A.; Trzebicka, B.; Momekova, D. Formulation and Evaluation of Hybrid Niosomal In Situ Gel for Intravesical Co-Delivery of Curcumin and Gentamicin Sulfate. *Pharmaceutics* **2022**, *14*, 747.
- (18) Bhardwaj, P.; Tripathi, P.; Gupta, R.; Pandey, S. Niosomes: A review on niosomal research in the last decade. *J. Drug Delivery Sci Technol.* **2020**, *56*, 101581.
- (19) Li, D.; Martini, N.; Wu, Z.; Chen, S.; Falconer, J. R.; Locke, M.; Zhang, Z.; Wen, J. Niosomal Nanocarriers for Enhanced Dermal Delivery of Epigallocatechin Gallate for Protection against Oxidative Stress of the Skin. *Pharmaceutics* **2022**, *14*, 726.
- (20) Fahmy, S. A.; Ramzy, A.; Mandour, A. A.; Nasr, S.; Abdelnaser, A.; Bakowsky, U.; Azzazy, H. M. E.-S. PEGylated Chitosan Nanoparticles Encapsulating Ascorbic Acid and Oxaliplatin Exhibit Dramatic Apoptotic Effects against Breast Cancer Cells. *Pharmaceutics* **2022**, *14*, 407.
- (21) Deitch, A. D.; Law, H.; deVere White, R. A stable propidium iodide staining procedure for flow cytometry. *J. Histochem Cytochem.* **1982**, *30*, 967–972.
- (22) Rao, K.; Roome, T.; Aziz, S.; Razzak, A.; Abbas, G.; Imran, M.; Jabri, T.; Gul, J.; Hussain, M.; Sikandar, B.; et al. Berberine loaded gum xanthan stabilized silver nanoparticles suppress synovial inflammation through modulation of the immune response and oxidative stress in adjuvant induced arthritic rats. *J. Mater. Chem. B* **2018**, *6*, 4486–4501.
- (23) Ekonomou, S. I.; Akshay Thanekar, P.; Lamprou, D. A.; Weaver, E.; Doran, O.; Stratakos, A. C. Development of Geraniol-Loaded Liposomal Nanoformulations against *Salmonella* Colonization in the Pig Gut. *J. Agric. Food Chem.* **2022**, *70*, 7004–7014.
- (24) Allam, A.; Fetih, G. Sublingual fast dissolving niosomal films for enhanced bioavailability and prolonged effect of metoprolol tartrate. *Drug Des. Dev. Ther.* **2016**, *10*, 2421–2433.
- (25) Bray, F.; Ferlay, J.; Soerjomataram, I.; Siegel, R. L.; Torre, L. A.; Jemal, A. Global cancer statistics 2018: GLOBOCAN estimates of incidence and mortality worldwide for 36 cancers in 185 countries. *CA: Cancer J. Clin.* **2018**, *68*, 394–424.
- (26) Rakha, E. A.; El-Sayed, M. E.; Green, A. R.; Lee, A. H. S.; Robertson, J. F. R.; Ellis, I. O. Prognostic markers in triple-negative breast cancer. *Cancer* **2008**, *118*, 1–17.
- (27) Ren, P.; Ren, X.; Cheng, L.; Xu, L. Frankincense, pine needle and geranium essential oils suppress tumor progression through the regulation of the AMPK/mTOR pathway in breast cancer. *Oncol. Rep.* **2017**, *39*, 129–137.
- (28) Mizuno, D.; Kawahara, M.; Konoha-Mizuno, K.; Yamazaki, K. Enhancing Cytotoxicity of Tamoxifen Using Geranium Oil. *Evid Based Complement Altern. Med.* **2022**, *2022*, 8091339.

- (29) Sant, D. W.; Mustafi, S.; Gustafson, C. B.; et al. Vitamin C promotes apoptosis in breast cancer cells by increasing TRAIL expression. *Sci. Rep.* **2018**, *8*, 5306.
- (30) Ashraf Ganjooei, N.; Ohadi, M.; Mostafavi, S. M. A.; Behnam, B.; Pardakhty, A. Preparing and assessing the physiochemical properties of curcumin niosomes and evaluating their cytotoxicity in 3T3 and MCF-7 cell lines. *Avicenna J Phytomed.* **2021**, *11*, 417–427.
- (31) Tomankova, K.; Polakova, K.; Pizova, K.; Binder, S.; Havrdova, M.; Kolarova, M.; Kriegova, E.; Zapletalova, J.; Malina, L.; Horakova, J.; Malohlava, J.; Kolokithas-Ntoukas, A.; Bakandritsos, A.; Kolarova, H.; Zboril, R. In vitro cytotoxicity analysis of doxorubicin-loaded/superparamagnetic iron oxide colloidal nanoassemblies on MCF7 and NIH3T3 cell lines. *Int. J. Nanomed.* **2015**, *10*, 949–961.
- (32) Imran, M.; Shah, M. R.; Ullah, F.; Ullah, S.; Sadiq, A.; Ali, I.; Ahmed, F.; Nawaz, W. Double-tailed acyl glycoside niosomal nanocarrier for enhanced oral bioavailability of Cefixime. *Artif. Cells Nanomed. Biotechnol.* **2017**, *45*, 1440–1451.
- (33) Parhi, P.; Mohanty, C.; Sahoo, S. K. Nanotechnology-based combinational drug delivery: An emerging approach for cancer therapy. *Drug Discovery Today* **2012**, *17*, 1044–1052.
- (34) Rajera, R.; Nagpal, K.; Singh, S. K.; Mishra, D. N. Niosomes: a controlled and novel drug delivery system. *Biol. Pharm. Bull.* **2011**, *34*, 945–953.
- (35) Moghassemi, S.; Hadjizadeh, A. Nano-niosomes as nanoscale drug delivery systems: an illustrated review. *J. Controlled Release* **2014**, *185*, 22–36.
- (36) Gharbavi, M.; Amani, J.; Kheiri-Manjili, H.; Danafar, H.; Sharafi, A. Niosome: A Promising Nanocarrier for Natural Drug Delivery through Blood-Brain Barrier. *Adv. Pharmacol. Sci.* **2018**, *2018*, 6847971.
- (37) Crowley, L. C.; Marfell, B. J.; Scott, A. P.; Waterhouse, N. J. Quantitation of Apoptosis and Necrosis by Annexin V Binding, Propidium Iodide Uptake, and Flow Cytometry. *Cold Spring Harb. Protoc.* **2016**, *2016*, pdb.prot087288.
- (38) Khazaei, S.; Esa, N. M.; Ramachandran, V.; Hamid, R. A.; Pandurangan, A. K.; Etemad, A.; Ismail, P. In vitro Antiproliferative and Apoptosis Inducing Effect of Allium atroviolaceum Bulb Extract on Breast, Cervical, and Liver Cancer Cells. *Front Pharmacol.* **2017**, *8*, 5.
- (39) Pires, A. S.; Marques, C. R.; Encarnacao, J. C.; Abrantes, A. M.; Mamede, A. C.; Laranjo, M.; Goncalves, A. C.; Sarmento-Ribeiro, A. B.; Botelho, M. F. Ascorbic acid and colon cancer: An oxidative stimulus to cell death depending on cell profile. *Eur. J. Cell Biol.* **2016**, *95*, 208–218.
- (40) Gomes, A.; Fernandes, E.; Lima, J. L. F. C. Fluorescence probes used for detection of reactive oxygen species. *J. Biochem. Biophys. Methods* **2005**, *65*, 45–80.
- (41) Kaur, N.; Sharma, I.; Kirat, K.; Pati, P. K. Detection of reactive oxygen species in *Oryza sativa* L.(rice). *Bio-Protoc.* **2016**, *6*, e2061–e2061.
- (42) Liu, Y.; Hong, H.; Lu, X.; Wang, W.; Liu, F.; Yang, H. L-ascorbic acid protected against extrinsic and intrinsic apoptosis induced by cobalt nanoparticles through ROS attenuation. *Biol. Trace Elem. Res.* **2017**, *175*, 428–439.